JOC Article

Synthesis of Novel Phthalocyanine−Tetrathiafulvalene Hybrids; Intramolecular Fluorescence Quenching Related to Molecular Geometry

Christopher Farren, Christian A. Christensen, Simon FitzGerald, Martin R. Bryce,* and Andrew Beeby*

Chemistry Department, University of Durham, South Road, Durham DH1 3LE, UK

m.r.bryce@durham.ac.uk; andrew.beeby@durham.ac.uk

Received May 17, 2002

A number of silicon phthalocyanine bis-esters have been synthesized and characterized, with axial ligands containing one or more tetrathiafulvalene groups. Variations in the substitution positions around a central aromatic "hinge" within the ligands lead to different molecular geometries, and the fluorescence of the macrocyclic core is subsequently quenched to varying degrees by the electron-rich tetrathiafulvalene moiety, the magnitude of this effect being dependent upon both the relative separation of the two units and the flexibility of the linking group. Pc derivative **24**, with a highly flexible linker group, and pc derivative **28**, with a dendritic axial ligand, have the intensity of the macrocycle emission reduced by 99% and 96%, respectively, relative to a similar silicon pc reference compound lacking the TTF moieties. Molecular modeling studies of a series of such hybrids allow the degree of this fluorescence quenching to be related to the intramolecular spacing. Additionally, the potential for rapid electrochemical switching of the phthalocyanine fluorescence by oxidation of the appended tetrathiafulvalene units is explored.

Introduction

Phthalocyanines (pcs) and their macrocyclic analogues continue to attract considerable attention, due in part to their characteristic optical properties,[1] and applications including medicinal therapeutic agents,[2] photosensitizers,[3] photoconductors,[4] catalysts,[5] and nonlinear optical devices[6] have been demonstrated. Despite the fact that many *peripherally* substituted pcs have been synthesized, with equatorial groups including ferrocenes,[7] crown ethers,[8] dendrimers,[9] solketal derivatives,[10] sugars,[11] and biologically "active" nucleobases,[12] there are relatively few *axially* substituted silicon pcs.[13] These macrocycles are not able to aggregate in solution and have higher quantum yields and fluorescence lifetimes than the more common zinc or aluminum pcs.[1b] Furthermore, pcs have long been known to undergo electron-transfer reactions, both to[14] and from[15] their excited states, and strong electron donors such as tetrathiafulvalene (TTF) are able to quench the pc fluorescence by *intermolecular* electron transfer.[16] We have previously described the synthesis of novel silicon pc bis-esters,[17] and we have now extended this methodology to produce new pc-TTF hybrids, which display *intramolecular* photoinduced electron-transfer processes.

Results and Discussion

Synthesis. In a previous article[17] we have described the synthesis of silicon phthalocyanine bis(4-*tert*-butyl)-benzoate **2** via the condensation of silicon pc dichloride

(1) Reviews: (a) Moser, F. H.; Thomas, A. L. *Phthalocyanine Compounds*; Reinhold: New York, 1963. (b) Leznoff, C. C., Lever, A. B. P., Eds. *Phthalocyanines, Properties and Applications*; VCH: New York, 1989−1996; Vols. 1−4. (c) McKeown, N. B. *Chem. Ind.* **1999**, 92.

(2) (a) Rosenthal, I. *J. Photochem. Photobiol.* **1991**, *53*, 859. (b) Panday, P. K.; Herman, C. K. *Chem. Ind.* **1998**, 739.

(3) (a) Nazeeruddin, M. K.; Humphry-Baker, R.; Gratzel, M.; Murrer, B. A. *Chem. Commun.* **1998**, 719. (b) Whitlock, J. B.; Panayotatos, P.; Sharma, G. D.; Cox, M. D.; Sauer, R. R.; Bird, G. R. *Opt. Eng.* **1993**, *32*, 1921. (c) Wohrle, D.; Meissner, D. *Adv. Mater.* **1991**, *3*, 129.

(4) Ahuja, R. C.; Hauffe, K. *Ber. Bunsen-Ges. Phys. Chem.* **1980**, *84*, 68 and references therein.

(5) (a) Parton, R. F.; Van Kelecom, I. F. J.; Bezoukhanova, M. J. A.; Jacobs, P. A. *Nature* **1994**, *370*, 541. (b) Lever, A. B. P.; Hempstead, M. R.; Leznoff, C. C.; Liu, W.; Melnik, M.; Nevin, W. A.; Seymour, P. *Pure Appl. Chem.* **1986**, *58*, 1467.

(6) Nalwa, H. S.; Shirk, J. S. In *Phthalocyanines, Properties and Applications*; Leznoff, C. C., Lever, A. B. P., Eds.; VCH: New York, 1996; Vol. 4, pp 83−181 and references therein.

(7) Cook, M. J.; Cooke, G.; Jafari-Fini, A. *J. Chem. Soc., Chem. Commun.* **1995**, 1715.

(8) (a) Van Nostrum, C. F.; Picken, S. J.; Schouten, A. J.; Nolte, R. J. M. *J. Am. Chem. Soc.* **1995**, *117*, 9957. (b) Van Nostrum, C. F.; Nolte, R. J. M. *Chem. Commun.* **1996**, 2385.

(9) (a) Brewis, M.; Clarkson, G. J.; Holder, A. M.; McKeown, N. B. *Chem. Commun.* **1998**, 1979. (b) Ng, A. C. H.; Li, X.-Y.; Ng, D. K. P. *Macromolecules* **1999**, *32*, 5292.

(10) Farren, C.; FitzGerald, S.; Beeby, A.; Bryce, M. R. *Chem. Commun.* **2002**, 572.

(11) Mallard, P.; Guerquin-Kern, J.-L.; Momenteau, M.; Gaspard, S. *J. Am. Chem. Soc.* **1989**, *111*, 9125.

(12) Li, X.-Y.; Ng, D. K. P. *Tetrahedron Lett.* **2001**, *42*, 305.

(13) McKeown, N. B. *J. Mater. Chem.* **2000**, *10*, 1979.

(14) Daraio, M. E.; Volker, A.; Aramendia, P. F.; San Roman, E. *Langmuir* **1996**, *12*, 2932.

(15) Darwent, J. R.; McCubbin, I.; Porter, G. *J. Chem. Soc., Faraday Trans. 2* **1982**, *78*, 903.

(16) Wang, C.; Bryce, M. R.; Batsanov, A. S.; Stanley, C. F.; Beeby, A.; Howard, J. A. K. *J. Chem. Soc., Perkin Trans. 2* **1997**, 1671.

(17) Farren, C.; FitzGerald, S.; Bryce, M. R.; Beeby, A.; Batsanov, A. S. *J. Chem. Soc., Perkin Trans. 2* **2002**, 59.

10.1021/jo020340y CCC: $22.00
Published on Web 11/21/2002

SCHEME 1

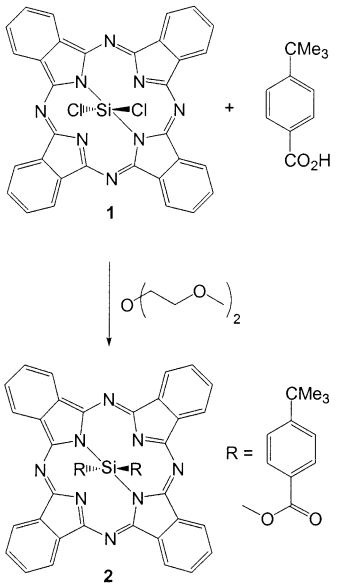

1 with the appropriate benzoic acid (Scheme 1). Due to its high solubility in organic solvents, and its relative stability in solution, **2** was used as a robust and reliable reference compound for previous photochemical studies, and this convention continues in the current work.

It is also known that (2-cyanoethyl)sulfanyl-substituted TTF derivatives **3a**−**c** can be used as nucleophilic building blocks,[18] and following the protocol of Becher et al.[19] we now demonstrate that deprotection of the hexyl-substituted TTF derivative **3c**[18c] with CsOH in DMF to generate the trialkylsulfanyl thiolate, followed by nucleophilic addition to methyl 4-bromomethylbenzoate produces **4** (Scheme 2) in good yield. In the present work our nomenclature uses a simple convention derived from three variables: benzene substitution point, relative to the benzoate group; number of atoms linking the two π-systems; and functionality on the benzene ring. Hence **4** is referred to as the para-2-ester. **4** was then hydrolyzed with sodium hydroxide in refluxing methanol/THF to give the para-2-acid **5** in essentially quantitative yield, and subsequent reaction with silicon pc dichloride **1** gave the first pc-TTF hybrid, **6** (i.e. para-2-pc).

Pc-TTF hybrid **6** is typical of axially substituted silicon pcs in that it gives characteristic ^{1}H NMR data,[17] the extensive macrocyclic ring current inducing a large *upfield* shift in the proton resonances of the proximal ligand hydrogen atoms. The four protons on the benzene ring in each of the two axial ligands thus give two distinct doublets at δ 5.04 and 6.18 ppm, respectively, compared to δ 7.41 and 8.05 ppm for the free benzoic acid **5**, and the pc *equatorial* hydrogen atoms give *downfield*-shifted resonances as unresolved multiplets at δ 8.4 and 9.7 ppm.

Having determined that the TTF-containing axial ligands in **6** reduce the pc fluorescence to under half that of the reference compound **2** (Table 1, photophysics are described in detail below), we synthesized pc-TTF hybrids

SCHEME 2

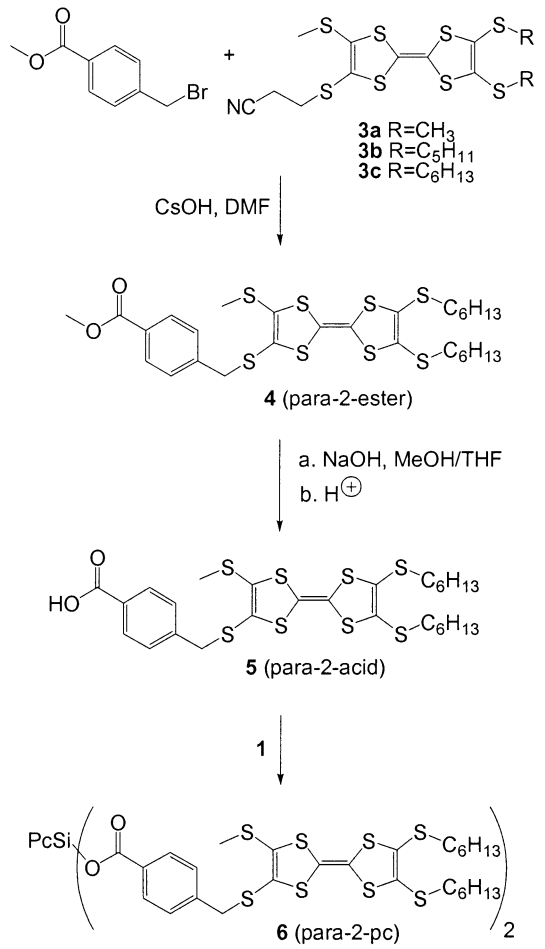

TABLE 1. Photophysical Data for pc-TTF Hybrid Systems

	τ_f/ns[a]				
	dichloromethane		2-methyltetrahydrofuran		
	τ_1 (yield)	τ_2 (yield)	τ_1 (yield)	τ_2 (yield)	Φ_f[b]
2	6.7 (100%)[c]		6.9 (100%)[c]		0.62 (100%)[e]
			6.9 (100%)[d]		
6	6.3 (93%)[c]	1.9 (7%)[c]	6.3 (94%)[c]	2.2 (6%)[c]	0.29 (47%)[e]
			6.8 (98%)[d]	2.2 (2%)[d]	
10	6.2 (91%)[c]	1.6 (9%)[c]	5.6 (86%)[c]	1.7 (14%)[c]	0.39 (63%)[e]
			6.5 (95%)[d]	2.2 (5%)[d]	
14	6.4 (91%)[c]	1.8 (9%)[c]	6.3 (92%)[c]	2.8 (8%)[c]	0.45 (73%)[e]
			6.5 (97%)[d]	2.1 (3%)[d]	
18	6.1 (96%)[c]	1.5 (4%)[c]	6.0 (88%)[c]	1.9 (12%)[c]	0.17 (27%)[e]
			6.5 (92%)[d]	2.7 (8%)[d]	
22	6.1 (92%)[c]	1.1 (8%)[c]	5.8 (95%)[c]	1.4 (5%)[c]	0.30 (48%)[e]
			6.3 (93%)[d]	1.7 (7%)[d]	
24			6.7 (93%)[d]	1.8 (7%)[d]	0.006 (1%)[e]
28			6.6 (92%)[d]	1.8 (8%)[d]	0.04 (6%)[e]

[a] ±0.1 ns, λ_{ex} = 635 nm, λ_{em} = 690 nm. [b] ±5%, λ_{ex} = 612 nm, λ_{em} = 640−800 nm, 293 K, dichloromethane. [c] 293 K. [d] 77 K. [e] % fluorescence relative to reference compound **2**.

with more flexible linking groups, to allow a greater interaction between the two π-systems. Methyl 4-hydroxybenzoate was thus reacted with an excess of 1,4-dibromobutane to give ester **7** (Scheme 3, n = 1). TTF derivative **3a**[18] was deprotected and subsequently reacted with **7** to give the para-6-ester **8**, and base hydrolysis to give the derived benzoic acid **9** followed by condensation

(18) (a) Lau, J.; Simonsen, O.; Becher, J. *Synthesis* **1995**, 521. (b) Simonsen, K. B.; Svenstrup, N.; Lau, J.; Simonsen, O.; Mørk, P.; Kristensen, G. J.; Becher, J. *Synthesis* **1996**, 407. (c) Christensen, C. A.; Bryce, M. R.; Becher, J. *Synthesis* **2000**, 1695.

(19) Simonsen, K. B.; Becher, J. *Synlett* **1997**, 1211.

SCHEME 3

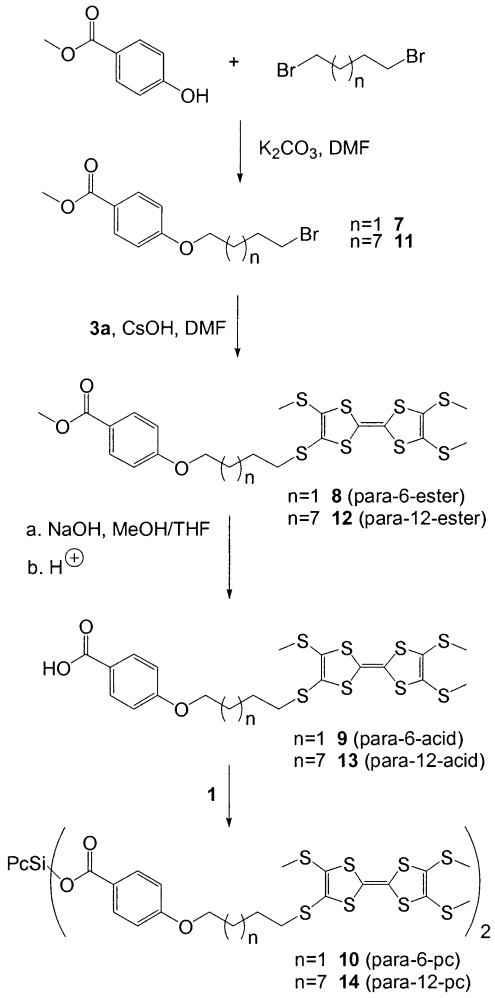

with silicon pc dichloride **1** gave pc-TTF hybrid **10** (i.e. para-6-pc). Similarly, methyl-4-hydroxybenzoate was reacted with 1,10-dibromodecane (n = 7), the TTF derivative **3a** was subsequently introduced, and hydrolysis and condensation gave the para-12-pc **14**, with a 12 atom chain linking the two π-systems.

Bis-esters **10** and **14** were characterized in a manner similar to **6**, and fluorescence measurements indicated that these two species displayed even less quenching of the pc emission, with the degree of quenching reducing with increasing linker group length. To more fully investigate this phenomenon, we repeated the synthesis using both 2- and 3-hydroxy-substituted methyl benzoates and 1,4-dibromobutane as the linking groups (Scheme 4). Thus were obtained pc bis-esters **18** and **22** (ortho-6-pc and meta-6-pc, respectively), and as the two π-systems are forced into closer proximity the interaction between them, and hence the quenching of the macrocycle emission, is increased.

All of the above pc-TTF hybrids have a benzoic acid group as the link to the pc core, as such pc bis-esters have been demonstrated to be chemically robust in both the solid state and solution under ambient conditions.[17] However, X-ray crystallography has shown that the benzene ring in such esters is held rigidly orthogonal to the plane of the macrocyclic core,[17] and will thus impose a certain minimum spacing between the pc and TTF

SCHEME 4

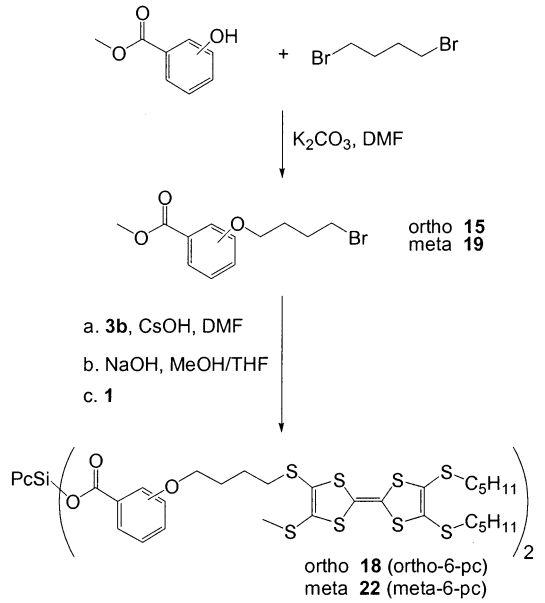

SCHEME 5

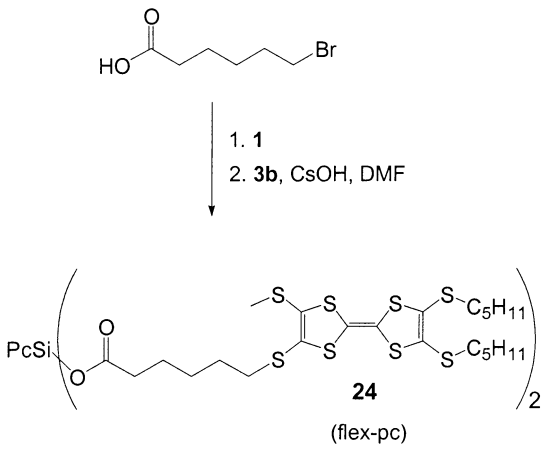

moieties in these compounds. We elected to synthesize a more flexible ligand, and the typical synthetic pathway was modified slightly. Silicon pc dichloride **1** was reacted with 6-bromohexanoic acid to give a bis bromoalkyl intermediate **23** (not shown) that was not characterized but reacted directly with **3b** to give hybrid **24** (Scheme 5). This compound showed dramatically reduced pc emission under a range of conditions, and our naming convention for this species is simply flex-pc.

Bis-ester **24**, however, was less stable in solution than the previous pc-TTF hybrids, presumably due to the increased steric accessibility of the Si−O bonds, and an alternative methodology was thus explored. To increase the local TTF concentration around the macrocyclic core, a TTF-containing dendritic species[18c] **25** (not shown) was reacted with methyl 4-(bromomethyl)benzoate (as in Scheme 2) to give ester **26**. Hydrolysis to the acid **27** and subsequent condensation gave the hybrid **28** (Scheme 6), which was stable in solution and which also had a greatly decreased macrocyclic emission intensity. Again, our naming convention uses simply dendrimer-ester, dendrimer-acid, and dendrimer-pc.

Photophysics. We have previously reported[17] the photophysical properties of our reference compound **2**, but

SCHEME 6

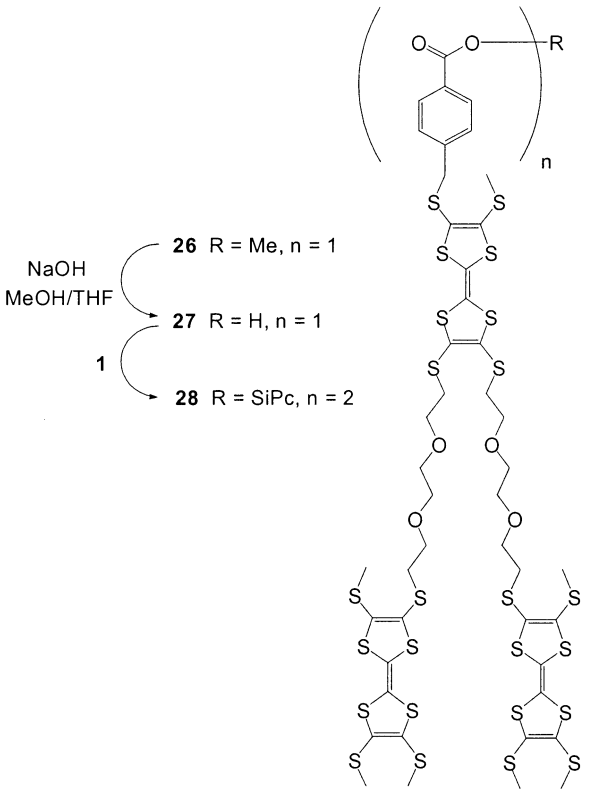

for clarity they are summarized here. The bulky axial ligands efficiently prevent aggregation in the concentration range 10^{-4}–10^{-7} mol dm^{-3} and sharply defined absorption and emission peaks are observed. As is typical for silicon pcs, the lifetime and quantum yield are increased with respect to the more commonly studied zinc and aluminum pcs[1b] (Table 1).

The electron-rich TTF moiety is known to be an efficient quencher of zinc pc emission by electron transfer, in both intermolecular and intramolecular mechanisms, the former with a rate constant of quenching $k_Q \approx 1 \times 10^{10}$ dm^3 mol^{-1} s^{-1}.[16] Similarly, we now show that **2** undergoes intermolecular quenching by TTF in dichloromethane with a rate constant of $k_Q = 1.6 \times 10^{10}$ dm^3 mol^{-1} s^{-1}. This result is not unexpected, but is useful in that it confirms that the presence of a central silicon atom and axial ligands does not perturb this propensity for pc fluorescence quenching by TTF.

The pc-TTF hybrid **6** shows a reduced quantum yield relative to reference compound **2**, equivalent to 53% quenching of the macrocycle fluorescence by the TTF electron donor. While this is a significant result, in comparison with the ≥95.5% intramolecular quenching exhibited by zinc pcs with four or eight peripheral TTF subsituents[16] the reduced efficiency of quenching in **6** was rather surprising. However, the crystal structure of **2** clearly shows the molecular rigidity of the benzoate units, which lie perpendicular to the plane of the macrocycle ring,[17] and the two atoms between the benzoate group and the TTF unit in **6** will add only minimal flexibility. Hence the reduced quenching in **6** is explained as being a direct consequence of the TTF moiety being held at a distance from the pc core. Compounds **10** and **14**, with added flexibility in the axial ligands (having linking groups consisting of 6 and 12 atoms, respectively) both display reductions in fluorescence quenching relative to **6**, with quantum yields of 0.39 and 0.45, respectively. It is apparent that the increase in linker length across the series **6** (2 atoms in a flexible unit), **10** (6 atoms), and **14** (12 atoms) has a direct effect upon the efficiency of quenching by TTF. Molecular modeling confirms that the increased flexibility in this series is more than offset by the concomitant increase in pc-TTF separation distance (Figure 1).

Fluorescence lifetimes for the three hybrids discussed so far all display a second minor component; the fluorescence decay of the reference compound **2** exhibits clear single-exponential behavior, and the presence of the quenching moiety in the pc-TTF hybrids seems to complicate matters. It is interesting to note that the *lifetimes* show no reduction in line with the reduced quantum yields. Similar behavior was noted for a thiophene-containing silicon phthalocyanine bis-ester,[17] and it is suggested that there are two possible states for these compounds: an *on* state in which fluorescence is observed with a normal lifetime and an *off* state in which fluorescence is rapidly and efficiently quenched, and for which the lifetime is very short. With *intermolecular* emission quenching, as displayed by reference compound **2** in the presence of TTF, this phenomenon is not observed, and fluorescence lifetime and quantum yield values decrease proportionally as quencher concentration increases.

In a further attempt to increase the quenching of the pc emission the ortho- and meta-substituted analogues of **10** were synthesized as detailed above. Enhanced quenching was observed for these two species, with **22** (meta) and **18** (ortho) possessing quantum yields of 0.30 and 0.17, respectively, the latter equivalent to 73% quenching of the pc emission by the axial TTF groups. Lifetimes were once again unperturbed by this quenching. However, it was apparent that despite being able to tune the degree of quenching by altering the ligand chain length and substitution pattern, the extent of quenching observed in the silicon pc bis-benzoate esters was far from that obtained with the peripherally substituted zinc pcs.

In contrast, compound **24**, without the rigid benzoate ester linkage, shows a dramatic increase in quenching relative to the previous compounds, and has a quantum yield of <0.006 indicating >99% of the excited state is quenched. That removal of the benzoate ester can result in such a profound change in behavior emphasizes just how rigid the benzoate ester group is in solution. Such efficient quenching provided a suitable system with which to investigate further the unusual two-state quenching model. The possibility of there being distinct *on* and *off* states for fluorescence led us to consider the effect of temperature upon the equilibrium between these two states. Cooling a solution of **24** (in 2-methyl-THF) to an optically transparent glass at 77 K resulted in a 300-fold increase in emission intensity,[20] exhibiting a sharp turn on below 125 K, coinciding with the glass point of the solvent (Figure 2). As the solvent solidifies the flexible ligand arm is frozen into its thermodynamically favored

(20) As cooling results in the sharpening of both absorption and emission spectra, and there is an increase in concentration as the solvent contracts, emission spectra were corrected for changes in absorption at the excitation point, and integrated emission spectra were used to calculate the reported increases in emission intensity.

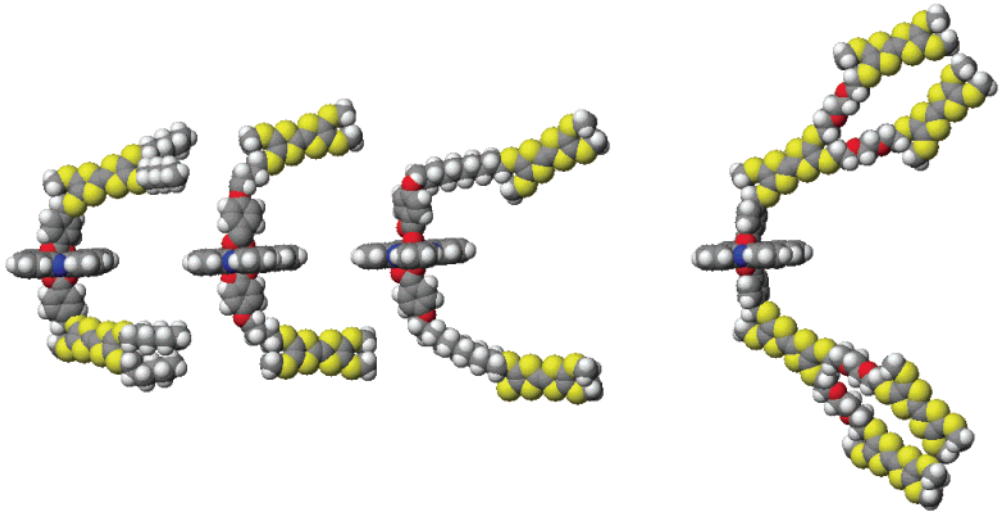

FIGURE 1. Energetically minimized structures of compounds **6**, **10**, **14**, and **28**, modeled using CAChe.

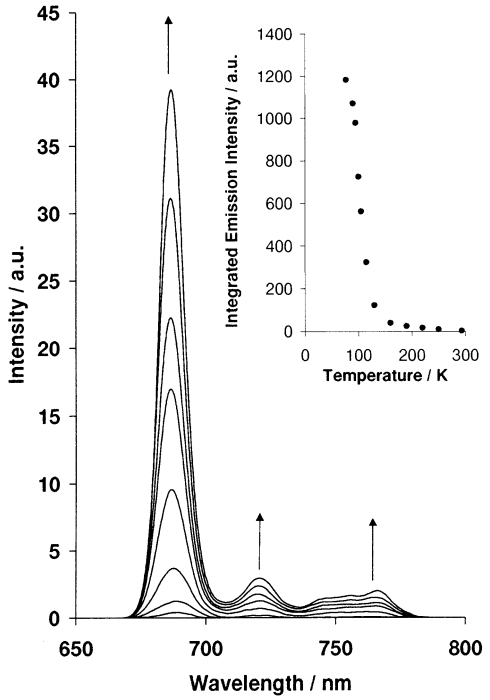

FIGURE 2. Temperature variation in emission of **24** in EPA solution, $\lambda_{ex} = 615$ nm. (Arrows indicate spectral changes with decreasing temperature.)

configuration, and the dramatic increase in emission indicates this to be with the TTF units held distant to the pc macrocycle. Similar temperature dependence of emission was observed for the other pc-TTF systems previously described, with the exception of **10** and **14**. These two compounds show the least fluorescence quenching at room temperature, and it is reasonable to suppose that with the TTF moiety already far removed from the pc core cooling has no further effect. The increase in emission of the other species can be directly related to their room-temperature quantum yields. Thus **24**, with the smallest quantum yield at 293 K, shows the largest increase on cooling, while compounds **6**, **22**, and **18** show more modest increases (1.5-, 2-, and 3-fold, respectively). The fluorescence lifetime of **24** was not measurable at room temperature, but was found to be 6.7 ns (plus a minor second component) at 77 K, this being similar to that of the reference **2**.

The dendritic species, **28**, despite the presence of the benzoate linker, showed similar emission properties to **24**, with a slightly larger quantum yield of 0.04 and correspondingly reduced effect on cooling to 77 K. An energy-minimized model of **28** is shown in Figure 1. The greater flexibility of the dendritic arms may allow, in dynamic solution, the outer TTF units to come into close proximity to the phthalocyanine core, resulting in enhanced quenching. Additionally, the increased local TTF concentration in **28** in comparison with **6**, **10**, and **14** would be expected to compound the quenching effect.

Electrochemistry and Spectroelectrochemistry. The electrochemistry of TTF is well-known,[21,22] and indeed cyclic voltametry of the para-2-pc compound **6** shows two clear and reversible one-electron TTF oxidation waves ($E^{1/2} = 0.23$ and 0.57 V, Figure 3). In addition, however, **6** also shows three clear one-electron waves from the pc core (one oxidation with $E^{1/2} = 0.78$ V and two reduction with $E^{1/2} = -0.98$ V and $E^{red} = -1.36$ V), and the overall voltamogram is significantly cleaner than the peripherally substituted pc-TTF hybrids we have reported previously.[16] In fact these species display almost ideal behavior, reflecting the reduced intermolecular interactions between the axially substituted pcs.

While TTF is an excellent electron donor, removal of one or two electrons to form the radical cation or dication species, respectively, imparts *acceptor* properties. The TTF first oxidation potential lies well below that of the pc core; hence it should be possible to selectively oxidize the TTF, thereby preventing it (in its oxidized form) from acting as an electron donor and quenching the pc emission. The result would be an electrochemically activated fluorescence switch comprising the nonfluorescent pc-TTF and fluorescent pc-$TTF^{+\bullet}$ species. Reversible formation of the TTF radical cation and dication can be followed spectroscopically,[23] and with an optically transparent thin

(21) Hunig, S.; Kiesslich, G.; Quast, H.; Scheutzow, D. *Liebigs Ann. Chem.* **1973**, 310.
(22) Reviews: (a) Bryce, M. R. *J. Mater. Chem.* **2000**, *10*, 589. (b) Segura, J. L.; Martin, N. *Angew. Chem., Int. Ed.* **2001**, *40*, 1372.

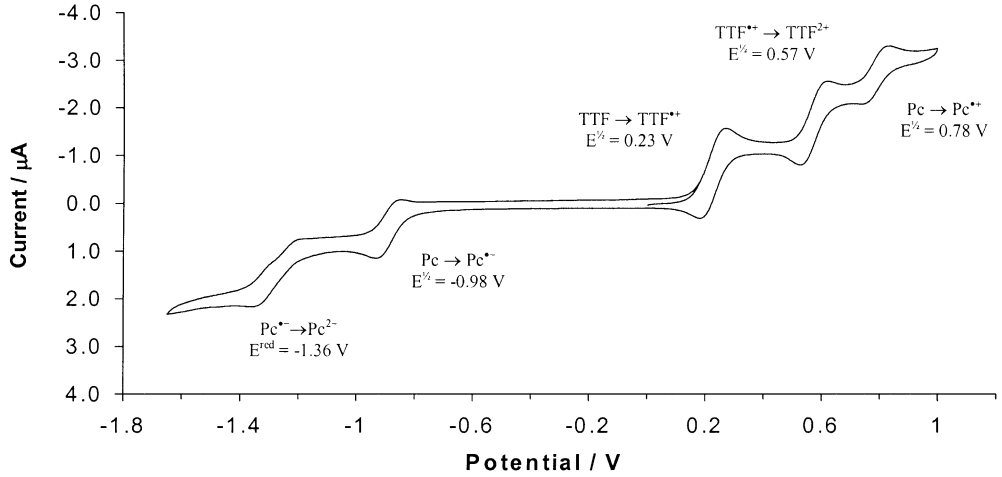

FIGURE 3. Cyclic voltamogram of **6** in DCM (vs $Ag/AgNO_3$, scan rate 20 mV/s, electrolyte = 0.1 M Me_4NBF_4).

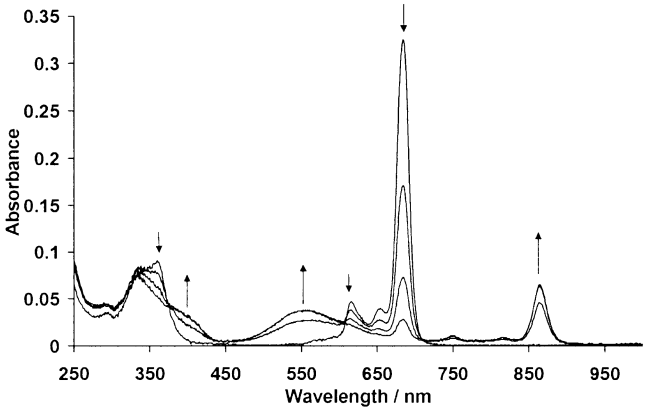

(Arrows indicate changes with increasing oxidation potential)

FIGURE 4. Absorbance changes from Pc → $Pc^{\bullet+}$ for **2** (electrolyte = 0.1 M Me_4NBF_4) (Arrows indicate changes with increasing oxidation potential.)

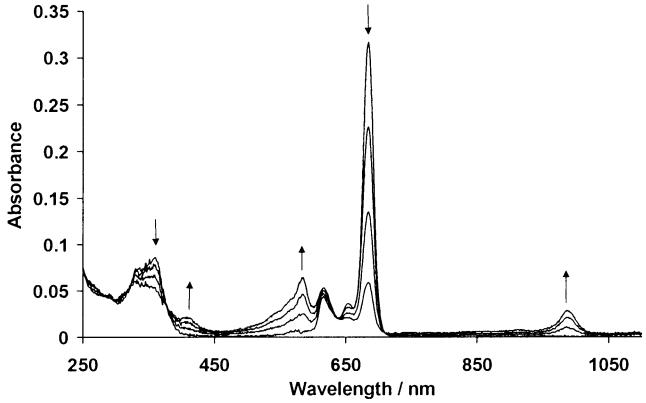

(Arrows indicate changes with increasing reduction potential)

FIGURE 5. Absorbance changes from Pc → $Pc^{\bullet-}$ (conditions as above, degassed by freeze−thawing). (Arrows indicate changes with increasing reduction potential.)

layer electrochemistry (OTTLE) cell developed for absorption and emission spectroscopy, we first studied the spectroelectrochemical behavior of the reference compound **2**.

Absorption spectra of phthalocyanine radical anions[24] and cations[25] are well-known, and both cationic and anionic pc radicals display loss of Q-band absorption with concomitant growth throughout the visible region. Reference compound **2** shows similar behavior, the radical cationic species displays transitions which can be assigned to three distinct regions: the B_1/B_2 envelope (300−450 nm), a $\pi \rightarrow \pi$ region (450−700 nm), and the Q-band region (750−900 nm) (Figure 4). Similarly, the radical anion shows new absorption bands at 410, 585, and 990 nm; the three regions described for the cation also apply here, albeit with the Q-band region extended to even lower energy, and the central area now assigned to $\pi^* \rightarrow \pi^*$ transitions (Figure 5).[24,25]

For all the pc-TTF compounds it was possible to achieve selective oxidation of the TTF group, apparent by new, broad absorption bands centered at 450 and 850 nm, which are assigned to the $TTF^{+\bullet}$ species.[23,26] The selectivity of oxidation was indicated by the pc Q-bands, which retained their shape and intensity throughout the reversible electrochemical process (Figure 6). The B_1/B_2 envelope does show a reduction in absorption, but this is due to removal of the overlapping TTF absorption (λ_{max} = 310 nm).

Emission spectra of the pc-TTF species were recorded in the OTTLE cell, but despite our selective oxidation of the TTF (as monitored by absorption spectroscopy) the pc emission spectrum remained unchanged. In theory, the observed quenching of the pc emission in the pc-TTF hybrids occurs via a simple electron-transfer process, from the TTF to the HOMO of the now excited pc* (Figure 7). Calculations based on Rehm−Weller theory[27] for electron transfer predict this to be a thermodynamically feasible process, both inter- and intramolecularly, and this is reflected in the observed and calculated rate constants (Table 2).

Photoexcitation of the pc increases its acceptor strength by an amount equal to the excitation energy (in this case

(23) Torrance, J. B.; Scott, B. A.; Welber, B.; Kaufman, F. B.; Seiden, P. E. *Phys. Rev. B* **1979**, *19*, 731.
(24) Mack, J.; Stillman, M. J. *J. Am. Chem. Soc.* **1994**, *116*, 1292.
(25) Ough, E.; Gasyna, Z.; Stillman, M. J. *Inorg. Chem.* **1991**, *30*, 2301.
(26) Khodorkovsky, V.; Shapiro, L.; Krief, P.; Shames, A.; Mabon, G.; Gorgues, A.; Giffard, M. *Chem. Commun.* **2001**, 2736.
(27) Rehm, D.; Weller, A. *Isr. J. Chem.* **1970**, *8*, 1982.

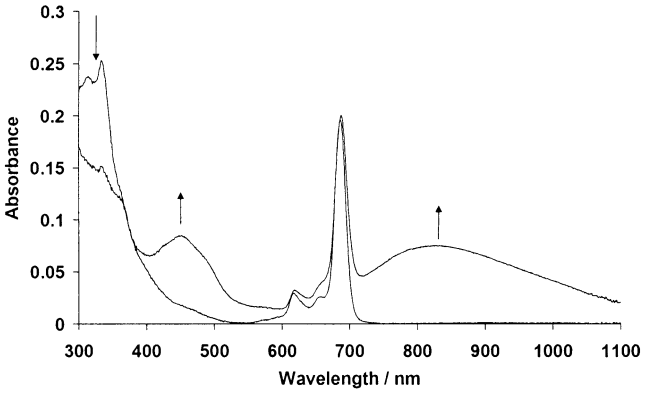

FIGURE 6. Spectroelectrochemistry of **28**, $E° = 0.5$ V. (Arrows indicate spectral changes upon oxidation of the TTF group.)

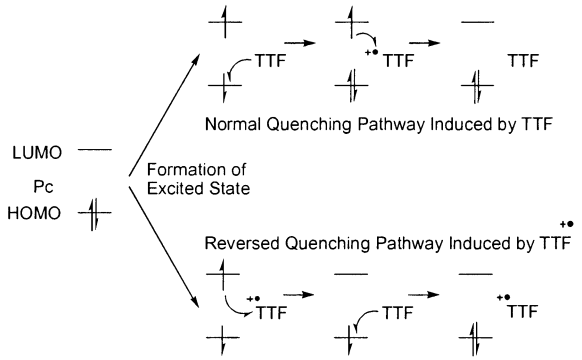

FIGURE 7. MO description of Pc emission quenching pathways.

1.81 eV) and hence electron transfer from TTF to pc* proceeds readily and results in emisson quenching. However, this increase in pc acceptor strength upon excitation is accompanied by an equal increase in *donor* strength, and thus pc* can readily donate electrons to electron-deficient species. The TTF radical cation is just such an electron-deficient species, and hence there exists a new, *reversed*, electron-transfer path, from pc* to $TTF^{+\bullet}$.

Thus oxidation of TTF in the pc-TTF hybrids does not result in an increase of fluorescence (reduction of quenching), and the Rehm−Weller calculations concur, yielding a quenching rate constant for this reverse process of 1.26×10^{10} dm^3 mol^{-1} s^{-1}. A similar phenomenon was reported by other workers during the preparation of this paper.[28] In their work enhanced fluorescence quenching of anthracene by $TTF^{+\bullet}$ in comparison with neutral TTF was observed, suggested to be due to increased binding between the electron-rich anthracene and the TTF radical cation. However, they do not discuss the nature of the electron-transfer process causing the quenching—although it is likely that the excited-state anthracene is quenched by the electron-deficient radical cation following a similar reversed electron-transfer pathway to that shown in Figure 7.

(28) De Cremiers, H. A.; Clavier, G.; Ilhan, F.; Cooke, G.; Rotello, V. M. *Chem. Commun.* **2001**, 2232.

Conclusions

A range of pc-TTF hybrids have been synthesized and characterized, the quenching of the pc emission by electron transfer from the axially linked TTF groups has been investigated, and the dependence of the quenching efficiency on the pc-TTF separation has been demonstrated. Variation of the axial ligand length and substitution position has resulted in pc-TTF hybrid systems with quantum yields ranging from 0.45 to 0.006, i.e., between 73% and <1% relative to a structurally similar reference compound **2** not containing the TTF moiety. The quenching is observed to be highly temperature dependent, with a sharp increase in emission at and below the glass point of the solvent, this being a result of the axial ligands being frozen into conformations where quenching is not favorable.

Spectroelectrochemistry of the reference compound shows absorption spectra for the pc radical anion and cation which are similar to previously reported examples. With the pc-TTF hybrid species, we have clearly demonstrated the possibility of selective oxidation to form pc-$TTF^{+\bullet}$ compounds. Interestingly, such species undergo fast electron transfer in the *reverse* direction to that of the unoxidized pc-TTF hybrids, and we thus present a facile method of reversing electron transfer within a donor−acceptor system.

Experimental Section

Synthesis. All solvents were dried by standard methodologies prior to use and silicon pc dichloride (**1**) was used as purchased (Fluka). While the "free" TTF-containing ligands were fully characterizable, many of the final pc-TTF hybrids did not give good mass spectra or elemental analysis but were deemed pure by NMR (see Supporting Information.)

Para-2-Ester (4). To a stirred solution of TTF derivative **3c**[18c] (568 mg, 1.00 mmol) in dry degassed DMF (40 mL) was added in one portion a solution of cesium hydroxide monohydrate (185 mg, 1.10 mmol) in dry degassed methanol (5 mL). The color of the mixture changed from orange to dark red and stirring was continued for 30 min. Methyl (4-bromomethyl)-benzoate (252 mg, 1.10 mmol) was added as a solid in one portion against a positive pressure of argon, causing the color to change back to orange. The reaction mixture was stirred for another 1 h before it was concentrated in vacuo. The residue was purified by column chromatography (silica gel, CH_2Cl_2−hexane 1:1 v/v) affording the para-2-ester **4** as an orange oil (649 mg, 98%). ^1H NMR (200 MHz, $CDCl_3$): δ 7.98 (2H, d, $J = 8.4$ Hz), 7.37 (2H, d, $J = 8.4$ Hz), 4.01 (2H, s), 3.91 (3H, s), 2.82 (4H, m), 2.21 (3H, br s), 1.63 (4H, m), 1.30 (12H, m), 0.86 (6H, t, $J = 6.6$ Hz). ^{13}C NMR (100 MHz, $CDCl_3$): δ 169.3, 143.0, 130.3, 128.9, 128.3, 51.9, 31.3, 31.2, 29.6, 28.0, 22.4, 19.0, 13.9. MS (EI^+) *m/z* (%): 662 (100, $[M]^+$) 378 (12), 149 (8), 121 (20). Anal. Calcd for $C_{28}H_{38}O_2S_8$: C, 50.68; H, 5.78. Found: C, 50.85; H, 5.84.

Para-2-Acid (5). Compound **4** (623 mg, 0.94 mmol) was dissolved in a mixture of dry tetrahydrofuran (15 mL) and dry methanol (15 mL), and sodium hydroxide (1.00 g, 25.0 mmol) was added as a solid in one portion. The reaction mixture was refluxed for 3 h in which time the sodium hydroxide had dissolved, whereupon it was concentrated under reduced pressure. The residue was taken into a mixture of water (100 mL) and dichloromethane (100 mL), and dilute hydrochloric acid (50 mL of a 0.5 M aqueous solution, 25.0 mmol) was added with stirring, making the aqueous phase colorless and the organic phase orange. The phases were separated and the organic phase was washed with water, dried ($MgSO_4$), and concentrated in vacuo to give the para-2-acid **5** as an orange

TABLE 2. Pc Emission Quenching Rate Constant Calculations

acceptor (E_{A/A^-}/V)	donor ($E_{D^+/D}$/V)	**a**[a] (nm)	ΔG (kJ mol^{-1})	$\Delta G^{\#}$ (kJ mol^{-1})	k_Q(calcd)[b] (dm^3 mol^{-1} s^{-1})	k_Q(exptl)[c] (dm^3 mol^{-1} s^{-1})
Pc (−0.69)	TTF (+0.59)	1	−66.4	1.47	1.14×10^{10}	1.6×10^{10}
		0.34	−96.1	1.03	1.20×10^{10}	
$TTF^{+\bullet}$ (+0.59)	Pc (+1.04)	0.34	−176	0.57	1.26×10^{10}	

[a] Encounter distance: 1 nm for an intermolecular process, 0.34 nm for an intramolecular process (calculated via models generated in CAChe). [b] Rate constant for quenching of phthalocyanine emission by TTF obtained via Rehm−Weller calculations. [c] Obtained for **2** via a Stern−Volmer plot.

glass (600 mg, 98%). Mp 91−92 °C. ^{1}H NMR (400 MHz, $CDCl_3$): δ 8.05 (2H, d, J = 8.0 Hz), 7.41 (2H, d, J = 8.4 Hz), 4.02 (2H, s), 2.82 (4H, m), 2.23 (3H, s), 1.64 (4H, pent, J = 6.8 Hz), 1.41 (4H, pent, J = 6.8 Hz), 1.30 (8H, m), 0.89 (6H, t, J = 6.4 Hz). ^{13}C NMR (100 MHz, $CDCl_3$): δ 171.5, 143.3, 130.5, 129.2, 128.3, 31.3, 31.3, 29.7, 28.2, 22.5, 19.1, 14.0. MS (EI$^+$) m/z (%): 648 (100, [M]$^+$) 513 (83), 378 (17), 135 (45). Anal. Calcd for $C_{27}H_{36}O_2S_8$: C, 49.96; H, 5.59. Found: C, 49.87; H, 5.61.

Para-2-Pc (6). Para-2-acid **5** (300 mg, 0.48 mmol) and silicon phthalocyanine dichloride **1** (100 mg, 0.16 mmol) were stirred together in di(methoxyethyl) ether (5 mL) at 160 °C for 6 h. Quenching of the reaction mixture in water (50 mL) and filtration of the resulting precipitate gave para-2-Pc **6** as a dark blue-green solid (134 mg, 46%) after column chromatography (silica gel, CH_2Cl_2). Mp >250 °C. ^{1}H NMR (400 MHz, $CDCl_3$): δ 9.71 (4H, m), 8.39 (4H, m), 6.18 (2H, d, J = 8.4 Hz), 5.04 (2H, d, J = 8.4 Hz), 3.32 (2H, s), 2.79 (2H, t, J = 7.6 Hz), 2.71 (2H, t, J = 7.6 Hz), 1.65 (3H, s), 1.56−1.25 (16H, m), 0.90 (3H, t, J = 7.6 Hz), 0.84 (3H, t, J = 7.6 Hz). ^{13}C NMR (100 MHz, $CDCl_3$): δ 158.9, 150.2, 139.8, 135.5, 132.9, 131.4, 129.5, 127.8, 127.7, 127.4, 127.3, 124.1, 123.1, 110.8, 109.0, 39.6, 36.3, 36.2, 31.3, 31.2, 29.7, 29.6, 28.2, 28.1, 22.6, 22.5, 18.4, 14.1, 14.0. (NMR in Supporting Information.)

Methyl 4-(4′-Bromobutoxy)benzoate (7). Methyl 4-hydroxybenzoate (1.00 g, 6.57 mmol), 1,4-dibromobutane (4.26 g, 19.72 mmol), and potassium carbonate (9.08 g, 65.70 mmol) were stirred in dry, degassed DMF (30 mL) for 24 h. The solvent was removed in vacuo and the residue taken up in CH_2Cl_2 and filtered. The filtrate was concentrated in vacuo and dried ($MgSO_4$), giving methyl 4-(4′-bromobutoxy)benzoate (**7**) as a white solid (1.55 g, 82%) after column chromatography (silica gel, CH_2Cl_2). Mp 42−43 °C. ^{1}H NMR (400 MHz, $CDCl_3$): δ 7.97 (2H, d, J = 8.8 Hz), 6.89 (2H, d, J = 8.8 Hz), 4.04 (2H, t, J = 6.0 Hz), 3.88 (3H, s), 3.49 (2H, t, J = 6.4 Hz), 2.07 (2H, m), 1.97 (2H, m). ^{13}C NMR (100 MHz, $CDCl_3$): δ 166.8, 162.56, 131.6, 122.6, 114.0, 67.0, 51.9, 33.3, 29.3, 27.7. MS (EI$^+$) m/z (%): 286/288 (25, [M]$^+$), 255/257 (10), 152 (25), 135/137 (94), 121 (100), 55 (93). Anal. Calcd for $C_{12}H_{15}BrO_3$: C, 50.19; H, 5.27. Found: C, 50.04; H, 5.26.

Para-6-Ester (8). Compound **3a**[18] (500 mg, 1.17 mmol), cesium hydroxide monohydrate (216 mg, 1.29 mmol), and methyl 4-(4′-bromobutoxy)benzoate (**7**, 336 mg, 1.17 mmol) were reacted as before, but in this case alkylation took 16 h. Purification by column chromatography (silica gel, CH_2Cl_2) afforded the para-6-ester **8** as a red oil, which solidified to an orange solid upon standing (634 mg, 93%). Mp 88−89 °C. ^{1}H NMR (400 MHz, $CDCl_3$): δ 7.99 (2H, d, J = 9.0 Hz), 6.91 (2H, d, J = 9.0 Hz), 4.05 (2H, t, J = 6.0 Hz), 3.90 (3H, s), 2.91 (2H, t, J = 7.0 Hz), 2.43 (9H, br s), 1.97 (2H, pent, J = 7.0 Hz), 1.85 (2H, pent, J = 7.0 Hz). ^{13}C NMR (100 MHz, $CDCl_3$): δ 166.79, 162.60, 131.54, 130.29, 127.40, 124.91, 122.47, 113.99, 110.74, 67.34, 51.83, 35.83, 27.76, 26.23, 19.19, 19.16. MS (EI$^+$) m/z (%): 580 (100, [M]$^+$), 373 (21), 238 (24), 165 (23), 121 (49), 91 (38). Anal. Calcd for $C_{21}H_{24}O_3S_8$: C, 43.42; H, 4.16. Found: C, 43.63; H, 4.19.

Para-6-Acid (9). Compound **8** (484 mg, 0.833 mmol) was treated with sodium hydroxide (1.00 g, 25.0 mmol) as before and subsequently neutralized using dilute hydrochloric acid to give the para-6-acid **9** as an orange solid (462 mg, 98%). Mp 139−140 °C. ^{1}H NMR (400 MHz, $CDCl_3$): δ 7.71 (2H, d, J = 9.0 Hz), 6.67 (2H, d, J = 8.8 Hz), 3.81 (2H, t, J = 6.0 Hz), 2.65 (2H, t, J = 7.2 Hz), 2.17 (9H, br s), 1.72 (2H, pent, J = 7.6 Hz), 1.59 (2H, pent, J = 7.6 Hz). ^{13}C NMR (100 MHz, $CDCl_3$): δ 168.36, 162.40, 131.44, 130.08, 127.04, 124.52, 122.23, 113.59, 110.21, 67.01, 35.32, 27.26, 25.82, 18.48, 18.40. MS (EI$^+$) m/z (%): 566 (100, [M]$^+$), 373 (23), 238 (32), 151 (24), 121 (29), 91 (33). Anal. Calcd for $C_{20}H_{22}O_3S_8$: C, 42.37; H, 3.91. Found: C, 42.73; H, 3.92. HRMS: $C_{20}H_{22}O_3S_8$ requires [M]$^+$, 565.9334. Found: [M]$^+$, 565.9330. Difference: 0.8 ppm.

Para-6-Pc (10). Para-6-acid **9** (280 mg, 0.49 mmol) and silicon phthalocyanine dichloride **1** (100 mg, 0.16 mmol) were reacted as above to give the para-6-Pc **10** as a dark blue-green solid (102 mg, 38%) after column chromatography over silica gel (eluent: CH_2Cl_2). Mp >250 °C; ^{1}H NMR (400 MHz, $CDCl_3$) δ 9.70 (4H, m), 8.38 (4H, m), 5.83 (2H, d, J = 8.4 Hz), 5.06 (2H, d, J = 8.4 Hz), 3.30 (2H, t, J = 7.6 Hz), 2.82 (2H, t, J = 7.2 Hz), 2.41 (3H, s), 2.38 (6H, s), 1.32 (4H, m). ^{13}C NMR (100 MHz, $CDCl_3$): δ 159.2, 150.1, 136.2, 133.4, 132.3, 130.7, 129.8, 127.2, 127.2, 126.1, 123.8, 122.5, 112.6, 110.9, 110.3, 66.2, 36.1, 30.6, 30.5, 29.5, 28.5, 19.1. Anal. Calcd for $C_{72}H_{58}N_8O_6S_{16}Si$: C, 51.71; H, 3.50; N, 12.96. Found: C, 51.48; H, 3.41, 12.82.

Methyl 4-(10-Bromodecyloxy)benzoate (11). Methyl 4-hydroxybenzoate (2.00 g, 13.15 mmol), 1,10-dibromodecane (11.83 g, 39.44 mmol), and potassium carbonate (18.17 g, 131.45 mmol) were reacted as before to give methyl 4-(10′-bromodecoxy)benzoate (**11**) as a white solid (4.19 g, 86%) after column chromatography (silica gel, CH_2Cl_2). Mp 64−65 °C. ^{1}H NMR (400 MHz, $CDCl_3$): δ 7.97 (2H, d, J = 9.2 Hz), 6.90 (2H, d, J = 9.2 Hz), 4.00 (2H, t, J = 6.4 Hz), 3.88 (3H, s), 3.41 (2H, t, J = 6.8 Hz), 1.82 (4H, m), 1.38 (12H, m). ^{13}C NMR (100 MHz, $CDCl_3$): δ 166.9, 162.9, 131.5, 122.3, 114.0, 68.1, 51.8, 34.1, 32.8, 29.4, 29.3, 29.3, 29.1, 28.7, 28.1, 25.9. MS (EI$^+$) m/z (%): 370/372 (30, [M]$^+$), 339/341 (4), 152 (100), 121 (69). Anal. Calcd for $C_{18}H_{27}BrO_3$: C, 58.22; H, 7.33. Found: C, 57.96; H, 7.42.

Para-12-Ester (12). Compound **3a**[18] (524 mg, 1.22 mmol), cesium hydroxide monohydrate (226 mg, 1.30 mmol), and methyl 4-(10′-bromodecoxy)benzoate (**11**, 336 mg, 1.17 mmol) were reacted as before, but again alkylation took 16 h. Purification by column chromatography (silica gel, CH_2Cl_2−hexane 2:1 v/v until excess alkylation reagent was off the column, then CH_2Cl_2) afforded the para-12-ester **12** as a yellow solid (802 mg, 98%). Mp 74−75 °C. ^{1}H NMR (400 MHz, $CDCl_3$): δ 7.97 (2H, d, J = 8.4 Hz), 6.90 (2H, d, J = 8.4 Hz), 4.00 (2H, t, J = 6.4 Hz), 3.88 (3H, s), 2.81 (2H, t, J = 6.4 Hz), 2.42 (9H, br s), 1.79 (2H, pent, J = 6.8 Hz), 1.63 (2H, pent, J = 6.8 Hz), 1.45−1.30 (12H, m). ^{13}C NMR (100 MHz, $CDCl_3$): δ 166.9, 162.9, 132.5, 129.3, 127.5, 127.4, 126.0, 122.3, 114.0, 68.1, 51.8, 36.3, 29.7, 29.4, 29.4, 29.3, 29.1, 29.0, 28.4, 26.0, 19.2, 19.2. MS (EI$^+$) m/z (%): 664 (100, [M]$^+$), 373 (9), 238 (15), 152 (12), 121 (25). Anal. Calcd for $C_{27}H_{36}O_3S_8$: C, 48.76; H, 5.46. Found: C, 48.99; H, 5.54.

Para-12-Acid (13). Compound **12** (670 mg, 1.01 mmol) was treated with sodium hydroxide (1.00 g, 25.0 mmol) as before and subsequently neutralized using dilute hydrochloric acid to give the para-12-acid **13** as a bright yellow powder (622 mg, 95%). Mp 120−121 °C. ^{1}H NMR (400 MHz, $CDCl_3$): δ 8.07 (2H, d, J = 9.0 Hz), 6.94 (2H, d, J = 9.0 Hz), 4.04 (2H, t, J = 6.5 Hz), 2.83 (2H, t, J = 7.5 Hz), 2.44 (9H, br s), 1.82 (2H, pent, J = 7.5 Hz), 1.65 (2H, pent, J = 7.5 Hz), 1.48−1.32 (12H, m). ^{13}C NMR (100 MHz, $CDCl_3$): δ 171.6, 163.6, 132.3, 129.3, 127.5, 127.4, 126.0, 121.3, 114.2, 68.2, 36.3, 29.7, 29.4, 29.4,

29.3, 29.1, 29.0, 28.4, 26.0, 19.2, 19.2. MS (EI$^+$) *m*/*z* (%): 650 (100, [M]$^+$), 388 (19), 308 (13), 238 (27), 138 (71), 121 (43). Anal. Calcd for $C_{26}H_{34}O_3S_8$: C, 47.96; H, 5.26. Found: C, 48.77; H, 5.38. HRMS: $C_{26}H_{34}O_3S_8$ requires [M]$^+$, 650.0274. Found: [M]$^+$, 650.0259. Difference: 2.3 ppm.

Para-12-Pc (14). Para-12-acid **13** (250 mg, 0.38 mmol) and silicon phthalocyanine dichloride **1** (100 mg, 0.16 mmol) were reacted as before to give *para-12-Pc* **14** as a dark blue-green solid (127 mg, 43%) after column chromatography (silica gel, CH_2Cl_2). Mp >250 °C. ^{1}H NMR (400 MHz, $CDCl_3$): δ 9.70 (4H, m), 8.37 (4H, m), 5.69 (2H, d, J = 8.8 Hz), 5.04 (2H, d, J = 8.8 Hz), 3.34 (2H, t, J = 6.8 Hz), 2.73 (2H, t, J = 7.2 Hz), 2.39 (3H, s), 2.38 (3H, s), 2.36 (3H, s), 1.05−1.56 (16H, m). ^{13}C NMR (100 MHz, $CDCl_3$): δ 161.0, 150.2, 135.6, 132.2, 131.2, 129.3, 129.2, 127.4, 127.4, 126.0, 124.0, 122.6, 112.4, 111.2, 110.3, 67.2, 36.2, 29.7, 29.6−28.3 (m), 25.6, 19.2. (NMR in Supporting Information.)

Methyl 2-(4′-Bromobutoxy)benzoate (15). Methyl 2-hydroxybenzoate (910 mg, 5.95 mmol), 1,4-dibromobutane (5.14 g, 23.80 mmol), and potassium carbonate (8.22 g, 59.47 mmol) were reacted as before to give *methyl* 2-(4′-bromobutoxy)-benzoate (**15**) as a colorless oil (1.22 g, 71%) after column chromatography (silica gel, CH_2Cl_2). ^{1}H NMR (400 MHz, $CDCl_3$): δ 7.77 (1H, d d, J = 7.6, 2.0 Hz), 7.43 (1H, t m, J = 7.8 Hz), 6.94 (2H, t, J = 7.6 Hz), 4.05 (2H, t, J = 6.0 Hz), 3.87 (3H, s), 3.51 (2H, t, J = 6.4 Hz), 2.11 (2H, m), 1.97 (2H, m). ^{13}C NMR (100 MHz, $CDCl_3$): δ 166.7, 158.2, 133.3, 131.6, 120.2, 120.2, 113.0, 67.6, 51.9, 33.6, 29.3, 27.6. MS (EI$^+$) *m*/*z* (%): 286/288 (5, [M]$^+$), 255/257 (3), 135/137 (31), 120 (100), 92 (49), 55 (86). Anal. Calcd for $C_{12}H_{15}BrO_3$: C, 50.19; H, 5.27. Found: C, 49.97; H, 5.34.

Ortho-6-Ester (16). To a solution of **3b** (synthesized in a manner analogous to **3a**) (540 mg, 1.00 mmol) in dry degassed DMF (40 mL) was added a solution of sodium methoxide (2.20 mL, 1.1 mmol of a 0.5 M solution in methanol) in one portion. The color of the mixture changed from orange to dark red and stirring was continued for 30 min. Compound **15** (316 mg, 1.10 mmol) was dissolved in dry degassed DMF (5 mL) and added to the reaction in one portion, causing the color to change back to orange. The reaction mixture was stirred for 16 h before it was concentrated in vacuo. The residue was purified by column chromatography (silica gel, CH_2Cl_2) affording the ortho-6-ester **16** as a sticky orange oil (674 mg, 97%). ^{1}H NMR (400 MHz, $CDCl_3$): δ 7.78 (1H, d m, J = 7.8 Hz), 7.44 (1H, t m, J = 7.8 Hz), 6.97 (2H, m), 4.06 (2H, t, J = 5.8 Hz), 3.88 (3H, s), 2.92 (2H, t, J = 7.2 Hz), 2.80 (4H, t, J = 7.2 Hz), 2.41 (3H, s), 1.95 (4H, m), 1.63 (4H, m), 1.36 (8H, m), 0.89 (6H, t, J = 6.8 Hz). ^{13}C NMR (100 MHz, $CDCl_3$): δ 166.8, 158.3, 133.4, 131.7, 129.9, 127.8, 125.3, 120.2, 113.1, 111.0, 109.6, 68.1, 52.0, 36.2, 35.9, 30.6, 29.4, 29.4, 27.8, 26.3, 22.2, 19.2, 14.0. MS (EI$^+$) *m*/*z* (%): 692 (100, [M]$^+$), 590 (5), 485 (5), 350 (7), 121 (13). Anal. Calcd for $C_{29}H_{40}O_3S_8$: C, 50.25; H, 5.82. Found: C, 50.20; H, 5.81.

Ortho-6-Acid (17). Compound **16** (549 mg, 0.792 mmol) was treated with sodium hydroxide (1.00 g, 25.0 mmol) as before and subsequently neutralized using dilute hydrochloric acid to give the ortho-6-acid **17** as a sticky orange oil (535 mg, 99%). ^{1}H NMR (400 MHz, $CDCl_3$): δ 8.18 (1H, d d, J = 7.8, $^4J_{HH}$ = 1.8 Hz), 7.55 (1H, t m, J = 8.4 Hz), 7.14 (1H, t, J = 7.8 Hz), 7.05 (1H, d, J = 8.4 Hz), 4.28 (2H, t, J = 6.4 Hz), 2.89 (2H, t, J = 6.8 Hz), 2.80 (4H, t, J = 6.8 Hz), 2.43 (3H, s), 2.10 (2H, pent, J = 7.6 Hz), 1.84 (2H, pent, J = 7.2 Hz), 1.63 (4H, m), 1.34 (8H, m), 0.89 (6H, t, J = 6.4 Hz). ^{13}C NMR (100 MHz, $CDCl_3$): δ 165.2, 157.3, 135.0, 133.8, 131.2, 125.9, 122.3, 117.7, 112.5, 69.5, 36.2, 30.6, 30.6, 29.4, 27.6, 25.8, 22.2, 19.1, 14.0. MS (EI$^+$) *m*/*z* (%): 678 (46, [M]$^+$), 556 (28), 500 (29), 338 (15), 138 (47), 120 (100). Anal. Calcd for $C_{28}H_{38}O_3S_8$: C, 49.52; H, 5.64. Found: C, 49.15; H, 5.57. HRMS: $C_{28}H_{38}O_3S_8$ requires [M]$^+$, 678.0587. Found: [M]$^+$, 678.0592. Difference: 0.8 ppm.

Ortho-6-Pc (18). Ortho-6-acid **17** (280 mg, 0.49 mmol) and silicon phthalocyanine dichloride **1** (100 mg, 0.16 mmol) were reacted as before to give ortho-6-Pc **18** as a dark blue-green solid (88 mg, 29%) after column chromatography (silica gel, CH_2Cl_2). Mp >250 °C. ^{1}H NMR (400 MHz, $CDCl_3$): δ 9.69 (4H, m), 8.37 (4H, m), 6.45 (1H, t, J = 8.5 Hz), 5.74 (3H, m), 3.23 (2H, t, J = 8.0 Hz), 2.94 (2H, t, J = 7.0 Hz), 2.79 (3H, s), 2.72 (4H, m), 1.74 (2H, pent, J = 8.0 Hz), 1.66 (2H, pent, J = 7.5 Hz), 1.38 (12H, m), 0.92 (6H, t, J = 7.2 Hz). ^{13}C NMR (100 MHz, $CDCl_3$); δ 158.6, 157.0, 150.0, 133.9, 131.6, 131.5, 130.0, 128.9, 127.0, 124.9, 123.8, 119.9, 117.3, 110.8, 109.4, 65.9, 35.8, 35.4, 30.8, 30.5, 29.3, 27.3, 26.6, 22.0, 19.0, 14.1. (NMR in Supporting Information.)

Methyl 3-(4′-Bromobutoxy)benzoate (19). Methyl 3-hydroxybenzoate (0.91 g, 5.95 mmol), 1,4-dibromobutane (5.14 g, 23.80 mmol), and potassium carbonate (8.22 g, 59.47 mmol) were reacted as before to give methyl 3-(4′-bromobutoxy)-benzoate (**19**) as a colorless oil (1.28 g, 75%) after column chromatography (silica gel, CH_2Cl_2). ^{1}H NMR (400 MHz, $CDCl_3$): δ 7.61 (1H, d m, J = 7.6 Hz), 7.53 (1H, t, J = 2.4 Hz), 7.32 (1H, t, J = 8.0 Hz), 7.07 (1H, d d m, J = 8.0, 2.4 Hz), 4.02 (2H, t, J = 6.0 Hz), 3.90 (3H, s), 3.48 (2H, t, J = 6.4 Hz), 2.06 (2H, m), 1.94 (2H, m). ^{13}C NMR (100 MHz, $CDCl_3$): δ 166.8, 158.7, 131.3, 123.3, 121.9, 119.8, 114.5, 66.9, 52.1, 33.3, 29.3, 27.7. MS (EI$^+$) *m*/*z* (%): 286/288 (17, [M]$^+$), 255/257 (11), 152 (37), 135/137 (98), 121 (100), 55 (86). Anal. Calcd for $C_{12}H_{15}BrO_3$: C, 50.19; H, 5.27. Found: C, 49.94; H, 5.23.

Meta-6-Ester (20). Compound **3b** (540 mg, 1.00 mmol) was deprotected using sodium methoxide as above (2.20 mL, 1.10 mmol of a 0.5 M solution in methanol) and alkylated using compound **19** (0.316 g, 1.10 mmol) over 16 h. Purification by column chromatography (silica gel, CH_2Cl_2) afforded the meta-6-ester **20** as an orange oil that solidified upon standing (671 mg, 97%). Mp 54−55 °C. ^{1}H NMR (400 MHz, $CDCl_3$): δ 7.64 (1H, d m, J = 7.5 Hz), 7.56 (1H, m), 7.35 (1H, t, J = 7.5 Hz), 7.10 (1H, d d m, J = 8.0, 3.0 Hz), 4.05 (2H, t, J = 6.0 Hz), 3.93 (3H, s), 2.92 (2H, t, J = 7.0 Hz), 2.82 (4H, m), 2.44 (3H, s), 1.97 (2H, pent, J = 7.5 Hz), 1.86 (2H, pent, J = 7.5 Hz), 1.64 (4H, m), 1.36 (8H, m), 0.91 (6H, t, J = 7.5 Hz). ^{13}C NMR (100 MHz, $CDCl_3$): δ 166.9, 158.8, 131.4, 130.2, 129.4, 127.7, 125.0, 122.0, 120.0, 114.5, 109.9, 67.4, 52.2, 36.2, 35.9, 30.6, 30.6, 29.4, 29.4, 27.9, 26.3, 22.2, 19.2, 14.0. MS (EI$^+$) *m*/*z* (%): 692 (100, [M]$^+$), 590 (5), 485 (5), 350 (7), 207 (11), 165 (14), 121 (20). Anal. Calcd for $C_{29}H_{40}O_3S_8$: C, 50.25; H, 5.82. Found: C, 50.04; H, 5.83.

Meta-6-Acid (21). Compound **20** (485 mg, 0.700 mmol) was treated with sodium hydroxide (1.00 g, 25.0 mmol) as before and subsequently neutralized using dilute hydrochloric acid to give the meta-6-acid **21** as an orange oil which solidified upon standing (438 mg, 92%). Mp 91−92 °C. ^{1}H NMR (400 MHz, $CDCl_3$): δ 7.64 (1H, d, J = 7.8 Hz), 7.54 (1H, br s), 7.30 (1H, t, J = 8.0 Hz), 7.08 (1H, d, J = 7.8 Hz), 3.95 (2H, m), 2.82 (6H, m), 2.44 (3H, s), 1.88 (4H, m), 1.64 (4H, m), 1.35 (8H, m), 0.91 (6H, t, J = 5.6 Hz). ^{13}C NMR (100 MHz, $CDCl_3$): δ 158.8, 130.2, 129.4, 127.7, 125.0, 122.6, 120.4, 114.9, 111.0, 109.6, 67.4, 36.2, 35.9, 30.6, 30.6, 29.4, 29.4, 27.9, 26.3, 22.2, 19.2, 14.0. MS (EI$^+$) *m*/*z* (%): 678 (100, [M]$^+$), 485 (7), 454 (10), 350 (11), 193 (14), 138 (20), 121 (29). Anal. Calcd for $C_{28}H_{38}O_3S_8$: C, 49.52; H, 5.64. Found: C, 49.26; H, 5.63.

Meta-6-Pc (22). Meta-6-acid **21** (280 mg, 0.49 mmol) and silicon phthalocyanine dichloride **1** (100 mg, 0.16 mmol) were reacted as before to give the meta-6-pc **22** as a dark blue-green solid (106 mg, 35%) after column chromatography (silica gel, CH_2Cl_2). Mp >250 °C. ^{1}H NMR (400 MHz, $CDCl_3$): δ 9.71 (4H, m), 8.39 (4H, m), 6.14 (2H, m), 4.85 (1H, m), 4.34 (1H, s), 4.23 (2H, t, J = 6.4 Hz), 2.76 (6H, m), 2.34 (3H, s), 1.55 (4H, m), 1.35 (12H, m), 0.88 (6H, m). ^{13}C NMR (100 MHz, $CDCl_3$): δ 159.0, 157.1, 150.2, 135.5, 131.7, 131.5, 130.0, 128.8, 127.7, 127.7, 125.1, 124.1, 119.9, 119.0, 110.9, 110.8, 66.1, 36.2, 35.7, 30.6, 30.6, 29.4, 29.4, 27.4, 26.0, 22.1, 19.1, 13.9. (NMR in Supporting Information.)

Flex-Pc (24). Silicon pc dichloride **1** (200 mg, 0.32 mmol) was reacted with 6-bromohexanoic acid (250 mg, 1.28 mmol) as above to give the derived bis-bromoalkyl substituted pc **23**. Excess hexanoic acid was removed by washing with hexane,

and the resulting blue solid was not purified but reacted with an excess of TTF derivative **3b** (517 mg, 0.96 mmol) as above to give the flex-pc **24** as a dark blue-green solid (56 mg, 10%) after column chromatography (silica gel, CH_2Cl_2). Mp >250 °C dec. ^{1}H NMR (400 MHz, $CDCl_3$): δ 9.71 (4H, m), 8.40 (4H, m), 2.79 (4H, m), 2.26 (3H, s), 2.09 (2H, t, J = 7.2 Hz), 1.62 (4H, m), 1.35 (8H, m), 0.85 (6H), 0.46 (2H, m), −0.62 (4H, m), −0.90 (2H, m). ^{13}C NMR (100 MHz, $CDCl_3$): δ 166.9, 150.0, 135.4, 131.4, 129.1, 129.0, 128.0, 126.1, 124.0, 110.8, 110.2, 38.2−13.9 (m). (NMR in Supporting Information.)

Dendrimer-Ester (26). The TTF-dendron **25**[18c] (1.192 g, 0.865 mmol) was deprotected using cesium hydroxide monohydrate (0.174 g, 1.04 mmol) as before and alkylated using methyl 4-bromomethylbenzoate (229 mg, 1.00 mmol). Purification by column chromatography (silica gel, CH_2Cl_2−EtOAc 98:2 v/v) afforded the dendrimer-ester **26** as a dark orange syrup (1.194 g, 94%). ^{1}H NMR (400 MHz, $CDCl_3$): δ 7.98 (2H, d, J = 8.4 Hz), 7.38 (2H, d, J = 8.4 Hz), 4.01 (2H, s), 3.91 (3H, s), 3.69 (16H, m), 3.01 (8H, q, J = 4.8 Hz), 2.42 (18H, br s), 2.23 (3H, s). ^{13}C NMR (100 MHz, $CDCl_3$): δ 129.9, 129.1, 124.4, 109.7, 70.5, 70.1, 52.2, 35.5, 19.2. MS (ES$^+$) m/z: 1472−1477 ([M]$^+$), 1493−1498 ([M + Na]$^+$), 1509−1513 ([M + K]$^+$). Anal. Calcd for $C_{46}H_{54}O_6S_{24}$: C, 37.27; H, 3.70. Found: C, 37.48; H, 4.08.

Dendrimer-Acid (27). Dendron **26** (1.140 g, 0.774 mmol) was treated with sodium hydroxide (1.00 g, 25.0 mmol) as above and subsequently neutralized using dilute hydrochloric acid to give the dendrimer-acid **27** as a dark red toffee (1.107 g, 98%). ^{1}H NMR (400 MHz, $CDCl_3$) δ 8.02 (2H, d, J = 8.2 Hz), 7.39 (2H, d, J = 8.2 Hz), 4.02 (2H, s), 3.73 (16H, m), 3.02 (8H, m), 2.43 (18H, br s), 2.27 (3H, s). ^{13}C NMR (100 MHz, $CDCl_3$): δ 168.8, 142.7, 134.7, 130.9, 130.3, 129.4, 128.3, 127.4, 70.5−70.1 (m), 35.4, 35.3, 19.2, 19.2. MS (ES$^+$) m/z: 1456−1460 ([M]$^+$), 1480−1486 ([M + Na]$^+$), 1495−1499 ([M + K]$^+$). Anal. Calcd for $C_{45}H_{52}O_6S_{24}$: C, 37.06; H, 3.59. Found: C, 37.47; H, 3.89.

Dendrimer-pc (28). Dendron **27** (597 mg, 0.41 mmol) and silicon phthalocyanine dichloride **1** (100 mg, 0.16 mmol) were reacted as above to give the dendrimer-pc **28** as a dark blue-green solid (183 mg, 33%) after column chromatography (silica gel, CH_2Cl_2). Mp >250 °C dec; ^{1}H NMR (400 MHz, $CDCl_3$): δ 9.71 (4H, m), 8.40 (4H, m), 6.18 (2H, d, J = 8.4 Hz), 5.05 (2H, d, J = 8.4 Hz), 3.63 (16H, m), 3.56 (2H, br s), 2.99 (8H, m), 2.38 (18H, br s), 2.17 (3H, s). (NMR in Supporting Information.)

Molecular Modeling. The computer program CAChe (v.5.02, Oxford Molecular, Ltd.) was used to perform structural optimization of the structures of the phthalocyanine compounds. The MM3 algorithm was used for the MOPAC structural optimizations, using the standard procedure for energy minimization.

Steady-State Spectroscopy. Background corrected UV−visible absorption spectra were recorded on an ATI Unicam UV/VIS UV2 spectrometer. Emission spectra were recorded on a Perkin-Elmer LS-50B luminescence spectrometer and were corrected for the spectral response of the machines. Fluorescence spectra were recorded under conditions carefully chosen to avoid the effects of reabsorption as described by Dhami et al.[29] Fluorescence quantum yields were recorded relative to Cresyl Violet in methanol (Φ_f = 0.54), and disulfonated aluminum pc in water (Φ_f = 0.40) using the method of Williams et al.[30]

Fluorescence Lifetimes Acquisition. The technique of time correlated single photon counting[31] was used to record fluorescence lifetimes of the phthalocyanine. All solutions under study were prepared with a concentration such that the maximum absorbance at the Q-band absorption was no greater than 0.05, to eliminate the effects of reabsorption.[29] The excitation source consists of a pulsed 635 nm diode laser (IBH NanoLED Model-02) providing output pulses of <200 ps at a repetition rate of 1 MHz. The fluorescence emission was collected at 90° to the excitation source, and the emission wavelength selected using a monochromator (Jobin Yvon Triax 190). The fluorescence was detected using a photomultiplier tube (IBH Model TBX-04) linked to a time-to-amplitude converter (Ortec 567) and multichannel analyzer (E. G. & G. Trump Card and Maestro for Windows v.5.10). The instrument response function (IRF) of the apparatus was measured using a dilute suspension of milk powder in water as a scattering medium giving an IRF with a duration of 450 ps full-width at half-maximum (fwhm). The time per channel was typically ∼50 ps, giving a full range of ∼50 ns over the 1024 point data set. All fluorescence decays were recorded to a minimum of 10 000 counts in the peak channel of the pulse height analyzer. The data were transferred to a computer and analyzed by using the standard method of iterative reconvolution and nonlinear least-squares fitting in a Microsoft Excel spreadsheet.[31] The quality of calculated fits was judged using statistical parameters including the Durbin−Watson parameter, reduced χ^2, random residuals, and autocorrelated residuals.

Spectroelectrochemistry. Spectroelectrochemical studies were performed using an optically transparent thin layer electrode (OTTLE) cell, comprising a 1 mm path length quartz cuvette, platinum mesh as the working electrode, and platinum wire reference and counter electrodes, as described elsewhere.[32] Absorption studies were achieved by passing the probe beam through the working electrode (and solution of interest). For fluorescence the cell was held at 45° to the excitation beam which was focused into the center of the cell. The emission was collected from the opposite side of the cell.

Acknowledgment. We gratefully acknowledge funding for C.F. and S.F. from the E.P.S.R.C. and funding for C.A.C. from the Danish Research Agency.

Supporting Information Available: ^{1}H and ^{13}C NMR spectra of compounds **6**, **14**, **18**, **22**, and **24** and the ^{1}H NMR spectrum of **28**. This material is available free of charge via the Internet at http://pubs.acs.org.

JO020340Y

(29) Dhami, S.; de Mello, A. J.; Rumbles, G.; Bishop, S. M.; Phillips, D.; Beeby, A. *Photochem. Photobiol.* **1995**, *61*, 341.
(30) Williams, A. T. R.; Winfield, S. A.; Miller, J. N. *Analyst* **1983**, *108*, 1067.
(31) O'Connor, D. V.; Phillips, D. *Time Correlated Single Photon Counting*; Academic Press: London, UK, 1984.
(32) Huff, C. M.; Heath, G. A. *Inorg. Chem.* **1991**, *30*, 2528.